# High-performance field-emission electron gun using a reticulated vitreous carbon cathode

Brady C. Smith,[a] Charles E. Hunt,[b] Ivor Brodie,[c] and Arthur C. Carpenter[d]
*Department of Electrical and Computer Engineering, University of California – Davis, One Shields Ave., Davis, California 95616*

(Received 25 August 2010; accepted 4 January 2011; published 25 January 2011)

Proof-of-concept experimental results stemming from beam simulations for a microfocus electron gun are presented. The simulations demonstrate the potential to produce 4 mA of current through a 40-$\mu$m-diameter spot, at an energy of 30 keV, emitted from a 1-mm-diameter cathode with low energy spread and high brightness. The experimental realization, scaled down for practicality, but consistent with and confirming the higher-energy simulation, produced 2 $\mu$A of current with an approximately 28 $\mu$m spot size at an energy of 9.3 keV. The electrons originated from an $Ar^+$-ion-treated reticulated vitreous carbon (RVC) field-emission cathode shaped as an approximately 1-mm-diameter disk. The primary application for this work is a highly monochromatic microfocus x-ray source for use in phase-contrast imaging, although other beam applications exist. The use of an $Ar^+$-ion-irradiated RVC cathode allows high, stable current at low electric field, superior to what is achievable using field-emitter arrays or carbon-nanotube cathodes. This method, scaled up to its maximum potential, also enables a high-current-density microfocus beam, which, to date, has not been demonstrated using thermionic cathodes. Such a beam applied to an x-ray source for phase-contrast imaging represents a significant benefit in medical diagnostics. © *2011 American Vacuum Society.* [DOI: 10.1116/1.3546032]

## I. INTRODUCTION

### A. Motivation

The motivation of this work is to develop a highly monochromatic microfocus x-ray source for use in phase-contrast imaging (XRPCI) applied to mammography. The phase-change cross-section for soft tissue such as breasts is three orders of magnitude higher than the absorption cross-section, which is currently applied for conventional medical imaging. Therefore, XRPCI offers great potential in increasing the density resolution of x-ray imaging.[1] Of the four basic experimental techniques for XRPCI, diffraction-enhanced imaging,[2] crystal interferometry,[3] grating interferometry,[4] and in-line holography,[5] the first three methods have modest diagnostic potential either due to very low thermal and vibrational tolerances (limiting them to a laboratory setting) or the requirement of a micropatterned grating (requiring small sample size). In-line holography, also known as refraction-enhanced imaging, is the realistic choice if a practical x-ray source, such as the target of this work, is ultimately developed.

Most XRPCI demonstrations have used synchrotron x-ray radiation passed through a monochromator. For XRPCI to have widespread medical applicability, a compact, less expensive, and more manufacturable x-ray source needs to be produced. Recently, Wu and Liu[5] specified the requirements for an electron-gun x-ray source applicable to in-line holography used for mammography. The estimates are that tube current should be 25 mA, to keep exposure time short, and spot size should be 25 $\mu$m (corresponding to $4 \times 10^3$ A/cm$^2$), to produce sufficient lateral spatial coherence for properly imaging tissue interfaces. The authors also suggest a Mo target with Mo- and Al-layer x-ray filters to achieve the desired level of monochromaticity. In this work we have used their specifications as our goal values.

### B. Gun design

The electron gun proposed here offers an improvement over the state of the art for producing a microfocus x-ray source. A field-emission mode of operation is chosen over thermionic emission. Advantages of field emission include elimination of the heat source, simple design, high reliability, higher current density, fast turn-on and turn-off times, and potentially lower energy spread.

Electron optical systems using thermionic cathodes typically image a crossover formed in front of the cathode.[6] They are limited by the maximum current density obtainable from the cathode, typically in a range 0.5–10 A/cm$^2$, and the energy spread of the electrons after the crossover. Since the brightness in the image cannot exceed that in the object, it has not been possible to meet the desired XRPCI specifications with thermionic-cathode materials. It has been confirmed[5] that this has been the major impediment to using thermionic-cathode microfocus x-ray sources for XRPCI, and has been the major incentive for exploring the field-emission alternative. A field-emission cathode can be imaged in a microfocus source without employing any crossover, thereby enabling a significantly brighter image.

[a]American Vacuum Society member; electronic mail: brcsmith@ucdavis.edu
[b]Electronic mail: hunt@ucdavis.edu
[c]Electronic mail: ibrodie@aol.com
[d]Electronic mail: accarpenter@ucdavis.edu

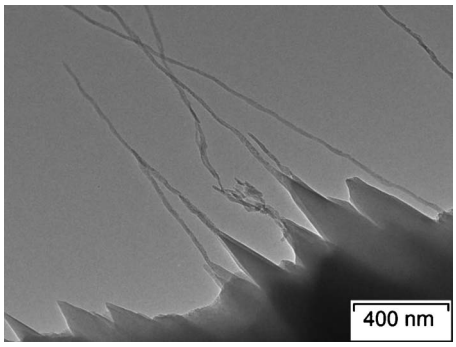


FIG. 1. TEM image of $Ar^+$-ion-irradiated RVC. This is a side view of a possible emissive surface showing mostly carbon cones and nanostructures created by the ion irradiation. The RVC matrix on which the nanostructures are grown is barely visible at the lower right. The high aspect ratio of the emissive structures and the direct attachment of nanowhisker structures to the RVC are seen.

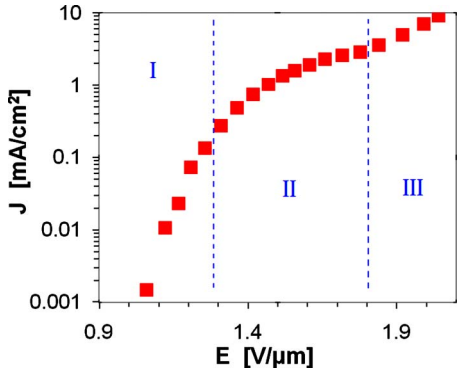


FIG. 2. (Color online) Measured current density $J(\mathrm{mA/cm^2})$ vs electric field $E(\mathrm{V}/\mu\mathrm{m})$ for a 3 mm diameter $Ar^+$-ion-irradiated RVC cathode. There are three regions of the graph as described at the end of Sec. I B.

Electron optical systems using single-tip field-emission sources avoid forming a crossover by imaging a submicron diameter source, which can have emission current densities exceeding $10^6$ $\mathrm{A/cm^2}$ to a submicron spot.[7] The effect of electron energy spread at the source on the electron-optical paths is essentially negligible. The total current from such a cathode is limited to values in the microampere range by the cathode heating to its melting point. Since the specified image diameter is 25 $\mu$m, we are imaging a random collection of nanometer-scale field emitters from which 25 mA can be obtained.

As a field-emission cathode material, carbon nanostructures have received a great deal of attention in recent years, partially because of high mechanical strength and chemical stability, and emission at low fields.[8–11] Additionally, the electrons emitted by carbon nanostructures are highly coherent, and if the structures, such as nanotubes, are randomly oriented initially, they bend to become aligned with a high electric field.[8] In the work presented here, the electron source chosen is a reticulated vitreous carbon (RVC) cathode that has been irradiated by $Ar^+$ ions to grow a large number of graphene-rich carbon nanostructures including single- and multiwalled carbon nanotubes (CNTs) distributed randomly over the already irregular surface of the RVC[12,13] (see Fig. 1). Measurements from this cathode, as in Fig. 2, have demonstrated the required current density at half of the electric field compared with other recent multiple-tip field-emission cathodes. In an electron gun, the electric fields and voltages can be half of the minimum possible with other macroscopic field-emission cathodes reported, resulting in higher total current without arcing. The emission pattern (projected on a phosphor screen) of a 3 mm diameter, 100 pores/in., $Ar^+$-ion-irradiated RVC cathode is shown in Fig. 3, illustrating (even with the blooming on the phosphor screen) that emission does, in fact, come from numerous tips. The cathode is also more robust than other field-emission cathodes since ion bombardment of the cathode during operation does not destroy the field-emission properties of the cathode, but, rather, *maintains* its excellent field-emission properties. This is because ion bombardment is responsible for the *self-assembly* of the graphene-rich carbon nanostructures themselves.[12] Another advantage of RVC is that the foamlike structure is resistively self-ballasting, mitigating bistable fluctuations in the field-emission process, normalizing current, and preventing damage. Comparison of the RVC cathode to a recent study using CNTs,[14] also for microfocus x-ray applications, reveals the above mentioned advantages of the treated RVC, particularly the low extraction field, indicating that the excellent results of that study can be improved further.

Note that in Fig. 2, the current density ($J$) versus electric field ($E$) behavior of $Ar^+$-ion-irradiated RVC does not obey the simple power or exponential increase in $J$ with $E$ observed for typical field-emission cathodes following the Fowler–Nordheim law. This is the consequence of RVC exhibiting partially semiconducting properties. The three regions of Fig. 2 have been explained as follows.[15] In region I, field emission follows the Fowler–Nordheim process, with the emitter tips having ample electron supply. Region II is characterized by depletion of electrons in the cathode material, limiting $J$. In region III, the fields within the cathode material are sufficient such that impact ionization restores electron supply in the material. Some authors have described carbon nanotubes as exhibiting these properties as well.[8]

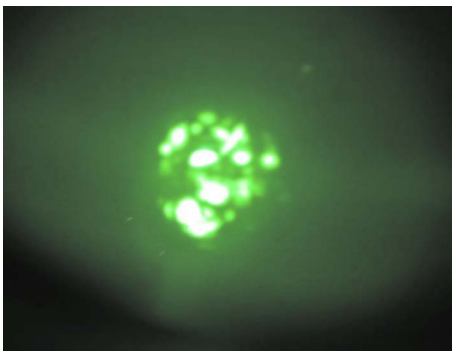

FIG. 3. (Color online) Emission pattern from a 3 mm diameter $Ar^+$-ion-irradiated RVC cathode imaged on a phosphor screen, demonstrating the numerous, randomly spaced emission sites.

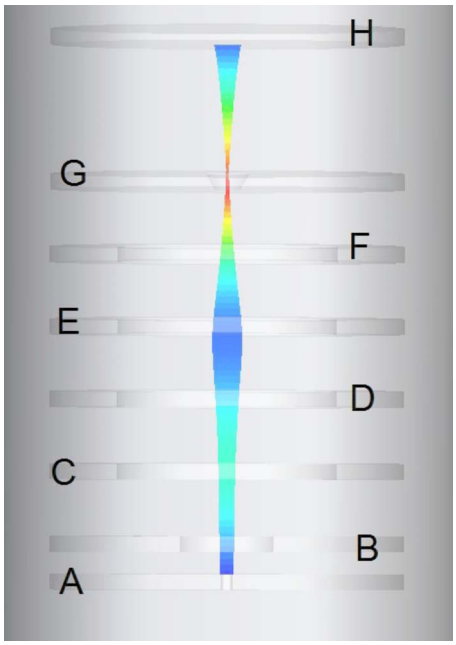


FIG. 4. (Color online) Simulation results of electrostatic focusing field-emission electron gun. The outer diameters of electrodes are 2.87 cm. The labeled terminals are as follows: A—"cathode" (0 V), B—"extraction1" (4 kV), C—"extraction2" (26 kV), D—"Einzel1" (7 kV), E—"Einzel2" (−14.1 kV), F—"Einzel3" (7 kV), G—"aperture" (30 kV), and H—"collector" (2.5 kV). In an x-ray source, the foil target would be fixtured at the aperture.

## II. MODELING

Using the $Ar^+$-irradiated RVC cathode, an electrostatically focusing electron gun has been designed as a proof-of-concept for applicability to an x-ray source. A cylindrically symmetric gun design is employed, with edge-rounded acceleration plates. Figure 4 shows a proof-of-principle simulation made using CST PARTICLE STUDIO.[16] The target x-ray foil would be positioned at terminal G, described as the "aperture." The electrons are emitted (bottom of the figure) from the RVC cathode, 1 mm in diameter. The Einzel lens has been designed with a very low center voltage to increase focusing power while reducing spherical aberration as much as possible.[17] The electric field established at the cathode is 2.795 $V/\mu m$. Comparing Fig. 2 with previous experimental data for single carbon nanotubes,[8] the individual carbon nanostructure currents are less than approximately 300 $\mu A$ in the proposed device. It is documented[18] that conventional thermally annealed CNTs fail at approximately 100 $\mu A$, predominantly by detachment of the tube. However, that value presumes the CNT is grown on a heterogeneous material, such as Ag, to facilitate nucleation of the tube. In our device, the carbon nanostructures are anchored, as can be seen in Fig. 1, to carbon through a cone of carbon, making use of the strong C–C bonds, and so have been demonstrated to emit much higher currents without detachment. Extrapolating from single nanotube data,[19] the energy spread at 300 $\mu A$ is less than approximately 1 eV. From other data,[20] we project (for purposes of our design simulation) that a shift in center energy of the CNT energy distributions from tip to tip (in multitipped cathodes) results in an additional energy spread of approximately 3 eV. For the purposes of the simulation, an energy spread of 4 eV and an emission angle randomly distributed between ±7° were assumed. In fact, the true emission angles for such high nanotube currents can reach ±45° or above, even for oriented emitters. However, at angles of emission beyond ±7°, the current per unit solid angle is small, and can be intercepted by the device's apertures. Practical, packaged devices would use a limiting aperture to exclude atypical electrons.

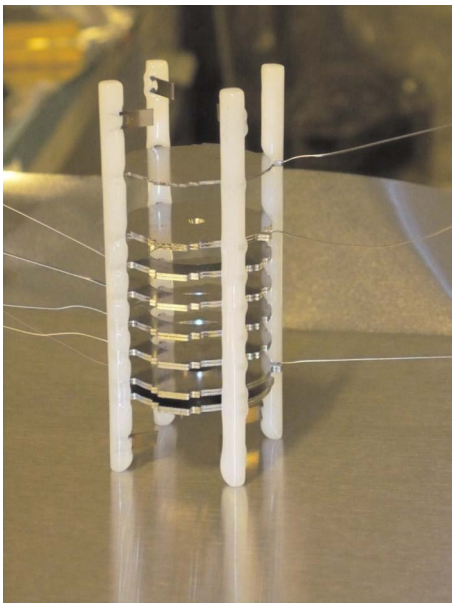

FIG. 5. (Color online) Photograph of the proof-of-concept electron gun, fabricated according to the parameters specified by the simulation in Fig. 4, for scaled-down operation in a vacuum system.

## III. EXPERIMENT

An experimental proof-of-concept electron gun was fabricated, as shown in Fig. 5. Stainless steel electrodes were used in a glass-rodded assembly, which was designed according to the simulations. One end of a cylinder of RVC was irradiated by $Ar^+$ ions for 30 min at an acceleration voltage of 1200 V and 200 mA current, to enhance its properties as a field emitter. This RVC material was then attached to the stainless steel cathode plate and electrically connected. To facilitate imaging the focal spot of the assembly, an 800 nm sheet of aluminum leaf was attached to the aperture (terminal G in Fig. 4), covering the aperture on the collector side. After operation, the aluminum was removed to observe the approximate beam profile. In an ion-pumped vacuum chamber below $10^{-6}$ torr, the assembly was operated at an aperture voltage of 9.3 kV. It was not possible to test the assembly at 30 kV due to (1) danger of intermittent arcs in the assembly, as fabricated, (2) the inability to image the beam with the Al-leaf method at the full acceleration potential, and (3) lack of available 30 kV supply resources. All terminal voltages were proportionally scaled. The scaled-voltage experiment is a reasonable proof-of concept, since

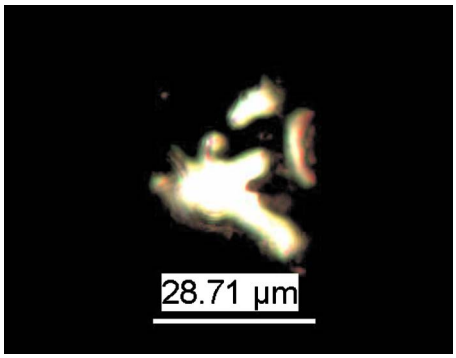


FIG. 6. (Color online) Bright-field transmission optical microscope image of holes in 800 nm thick Al leaf, produced by the electron beam at the focus of the electron gun in Fig. 5.

(by the electrostatic principle) the scaling should not significantly alter the focusing properties. Simulation was repeated at the lower electrode potentials to verify this. The gun was operated steady-state for 5 min to ensure ablation of the 800 nm thick aluminum.

## IV. RESULTS AND DISCUSSION

The simulated current in the electron gun was approximately 4 mA, using cathode performance extrapolated from the experimental data of Fig. 2. The energy spread at the source increased the spot size slightly (as compared to the design specification) to 30 $\mu$m. With full angular distribution of electrons (neglecting any limiting aperture) at the cathode included, the spot size increased to 40 $\mu$m, confirming the benefit of including a limiting aperture in commercial realizations. The maximum electric fields around the electrodes barely exceeded 10 V/$\mu$m, indicating that vacuum breakdown should not be a problem. Spherical and chromatic aberration coefficients (referred to the image) were simulated to be $C_{si}=60$ cm and $C_{ci}=53$ cm, respectively. Normalized to the radius of the openings in most of the electrodes, the figures of merit are then $C_{si}/R=33$ and $C_{ci}/R=30$, where $R$ is the radius of these openings. Simulation at the proportionally scaled-down voltages of the experiment yielded almost identical electron paths, as expected.

The experimental device performed slightly better than the simulations would suggest. The measured beam current was 2 $\mu$A, slightly better than expected from the data of Fig. 2. The spot size, as shown in the transmission optical microscope image of the Al leaf, as seen in Fig. 6, was less than the expected 40 $\mu$m. The irregular shape seen in Fig. 6 is expected, given that this is the image of the irregular emission from the RVC. Such a spot shape, however, would not adversely affect an x-ray source. Some variability was expected, considering that when using this hand-shaped RVC cathode, which was also hand-fitted in the assembly, the gun would not perform as would be expected from a precision machined and fitted production part. The shape of the spot imaged in the aluminum leaf corresponds reasonably to the shape of the RVC cathode, optically observed after the experiment. Estimating that at least 30% of the cathode was emitting (a value that agrees with earlier measurements in RVC)[21] a beam diameter reduction factor of at least 10 was achieved, even without any device optimization. The performance, both in current density and absolute spot size, could be optimized using the beam interception characterization method, but this was not possible with the proof-of-concept experimental fixture of Fig. 5. Optimizations in terminal voltages, dictated by measurements, would likely overcome the inherent limitations of simulations. In this experiment, pure simulation results were used to design and operate the gun, without any adjustments.

Implementations of this electron gun, with a RVC cathode in an x-ray source, would employ a Mo foil target [and ultimately, with acceleration up to 60 keV to maximize the (monochromatic) characteristic x-ray radiation, as would be beneficial to XRPCI, and increase total x-ray yield].[22] In an x-ray tube for XRPCI, using the x rays antiparallel to the electron beam direction optimizes monochromaticity versus bremsstrahlung, as well.[23] The characteristic photon flux would be $5\times10^9$ photons $sr^{-1}$ $s^{-1}$ or higher, for a 25 mA electron beam and a 100 nm Mo foil thickness.[23] This potential appears feasible using the method discussed here, and such results, which have not been achievable using thermionic sources, would make XRPCI practical.

Other applications of this microfocus field-emission source include microwave traveling-wave tube power amplifiers, klystrons, gyrotrons, free electron lasers, triodes, pentodes, terahertz radiation emission sources, Compton profile analysis, x-ray diffraction, x-ray fluorescence, and calibration of dosimeters. In medical applications, coherent-scatter computer-aided tomography (CT) and fluorescence-based molecular imaging in CT may also benefit from this method. The use of monochromatic x rays in medicine, in general, reduces the necessary patient dose by up to a factor of 4.[24]

## V. SUMMARY AND CONCLUSIONS

A field-emission electron gun has been designed, simulated, and implemented in a proof-of-concept form. Simulations indicate that a 4 mA current through a 40 $\mu$m diameter spot at 30 keV electron energy is achievable. This is applicable to x-ray sources used for phase-contrast imaging. Scaled 9.3 kV experimental results produced 2 $\mu$A of current through a less than 30 $\mu$m diameter spot. The spherical and chromatic aberration coefficients (referred to the image) of the electron gun are estimated to be $C_{si}=60$ cm and $C_{ci}=53$ cm, respectively. The experimental results suggest that a gun of comparable design, upscaled for operation at 30 keV, is feasible. This work represents initial verification that high-current, microfocus, field-emission-cathode electron guns may enable practical x-ray phase-contrast imaging sources. Other applications of the technology are also identified.

## ACKNOWLEDGMENT

The authors would like to thank Hans W. P. Koops of HaWilKo GmbH for his advice on electron optics and other topics.

[1]R. A. Lewis *et al.*, Br. J. Radiol. **76**, 301 (2003).
[2]T. J. Davis, D. Gao, T. E. Gureyev, A. W. Stevenson, and S. W. Wilkins, Nature (London) **373**, 595 (1995).
[3]A. Momose, T. Takeda, Y. Itai, A. Yoneyama, and K. Hirano, J. Synchrotron Radiat. **5**, 309 (1998).
[4]T. Weitkamp, C. David, O. Bunk, J. Bruder, P. Cloetens, and F. Pfeiffer, Eur. J. Radiol. **68**, S13 (2008).
[5]X. Wu and H. Liu, Med. Phys. **30**, 2169 (2003).
[6]H. Moss, *Narrow Angle Electron Guns and Cathode Ray Tubes* (Academic, New York, 1968), p. 3.
[7]A. V. Crewe, D. N. Eggenberger, J. Wall, and L. M. Welter, Rev. Sci. Instrum. **39**, 576 (1968).
[8]W. Zhu, *Vacuum Microelectronics* (Wiley, New York, 2001), p. 265.
[9]N. S. Xu and S. E. Huq, Mater. Sci. Eng. R. **48**, 47 (2005).
[10]D. S. Y. Hsu and J. L. Shaw, J. Appl. Phys. **98**, 014314 (2005).
[11]N. de Jonge, M. Allioux, J. T. Oostveen, K. B. K. Teo, and W. I. Milne, Phys. Rev. Lett. **94**, 186807 (2005).
[12]C. E. Hunt, A. G. Chakhovskoi, and Y. Wang, J. Vac. Sci. Technol. B **23**, 731 (2005).
[13]A. C. Carpenter, MS thesis, University of California, 2009.
[14]X. Calderón-Colón, H. Geng, B. Gao, L. An, G. Cao, and O. Zhou, Nanotechnology **20**, 325707 (2009).
[15]D. K. Schroder, R. N. Thomas, J. Vine, and H. C. Nathanson, IEEE Trans. Electron Devices **21**, 785 (1974).
[16]CST PARTICLE STUDIO, simulator produced by Computer Simulation Technology AG, Darmstadt, Germany.
[17]M. Szilagyi, *Electron and Ion Optics* (Plenum, New York, 1988), p. 352.
[18]E. Minoux *et al.*, Nano Lett. **5**, 2135 (2005).
[19]T. Fujieda, M. Okai, and H. Tokumoto, Jpn. J. Appl. Phys. **47**, 2021 (2008).
[20]M. J. Fransen, T. L. van Rooy, and P. Kruit, Appl. Surf. Sci. **146**, 312 (1999).
[21]J. R. Chacon, Ph.D. thesis, University of California, 2008.
[22]N. A. Dyson, Phys. Med. Biol. **20**, 1 (1975).
[23]G. Harding, B. David, A. Harding, A. Thran, and J. P. Schlomka, Radiat. Phys. Chem. **76**, 1116 (2007).
[24]G. Harding, B. Schweizer, G. Martens, J.-P. Schlomka, and A. Thran, Proc. SPIE **5199**, 193 (2004).